LIMNOLOGY and OCEANOGRAPHY

ASLO

Limnol. Oceanogr. 9999, 2024, 1–14

doi: 10.1002/lno.12641

Impact of aggregate-colonizing copepods on the biological carbon pump in a high-latitude fjord

Camilla Svensen [1*] **Morten Iversen** [2,3] **Fredrika Norrbin** [1] **Klas Ove Möller** [4] **Ingrid Wiedmann** [1] **Jofrid Skarðhamar** [5] **Coralie Barth-Jensen** [1] **Slawomir Kwasniewski** [6] **Mateusz Ormanczyk** [6] **Anna Maria Dąbrowska** [5] **Marja Koski** [7]

[1]Department of Arctic and Marine Biology, UiT the Arctic University of Norway, Tromsø, Norway
[2]Alfred Wegener Institute for Polar and Marine Research, Bremen, Germany
[3]MARUM and University of Bremen, Bremen, Germany
[4]Institute of Carbon Cycles, Helmholtz-Zentrum Hereon, Geesthacht, Germany
[5]Institute of Marine Research, Tromsø, Norway
[6]Department of Marine Ecology, Institute of Oceanology Polish Academy of Sciences, Sopot, Poland
[7]Technical University of Denmark, Lyngby, Denmark

Abstract

Zooplankton consumption of sinking aggregates affects the quality and quantity of organic carbon exported to the deep ocean. Increasing laboratory evidence shows that small particle-associated copepods impact the flux attenuation by feeding on sinking particles, but this has not been quantified in situ. We investigated the impact of an abundant particle-colonizing copepod, *Microsetella norvegica*, on the attenuation of the vertical carbon flux in a sub-Arctic fjord. This study combines field measurements of vertical carbon flux, abundance, and size-distribution of marine snow and degradation rates of fecal pellets and algal aggregates. Female *M. norvegica* altered their feeding behavior when exposed to aggregates, and ingestion rates were 0.20 μg C ind.$^{-1}$ d^{-1} on marine snow and 0.11 μg C ind.$^{-1}$ d^{-1} on intact krill fecal pellets, corresponding to 48% and 26% of the females' body carbon mass. Due to high sea surface abundance of up to $\sim$ 50 ind. L^{-1}, the population of *M. norvegica* had the potential to account for almost all the carbon removal in the upper 50 m of the water column, depending on the type of the aggregate. Our observations highlight the potential importance of abundant small-sized copepods for biogeochemical cycles through their impact on export flux and its attenuation in the twilight zone.

The quantity of carbon that leaves the surface ocean and its attenuation deeper down in the water column depends primarily on the balance between the carbon production and carbon remineralization. Large and dense particles such as fecal pellets and marine snow are generally important contributors to the carbon export (Fowler and Knauer 1986). While fecal pellets are produced by zooplankton as rather well-defined particles, marine snow, defined as organic particles > 500 μm in equivalent spherical diameter (Alldredge and Silver 1988), are formed when smaller particles collide and stick together (Alldredge and Jackson 1995). Marine snow are particles of various shapes and usually difficult to describe systematically (but *see* Trudnowska et al. 2023) and may represent an important food source (Green and Dagg 1997; Cawley et al. 2021). A majority of the particles produced in surface ocean are therefore degraded and remineralized by microbes (Steinberg et al. 2008) and zooplankton (Turner 2002) and never reach the sea floor. Most of the vertical flux attenuation takes place in the upper 100 m, where the concentration of mesozooplankton is high and particle degradation by feeding copepods is important (Iversen 2023). Microbial degradation of sinking particles is equally important in deeper water, where the mesozooplankton concentration is low (Iversen et al. 2010; Iversen 2023).

*Correspondence: camilla.svensen@uit.no

Additional Supporting Information may be found in the online version of this article.

Author Contribution Statement: CS conceived the study and drafted the first manuscript with contributions from MI and MK. CS, MI, FN, KOM, IW, and JS contributed to sampling design, data collection, and analyzes. MK designed and conducted feeding experiments and analyzed the data. MO, SK, and CB-J analyzed the zooplankton samples and AMD analyzed the protist samples. All authors contributed to interpretation of the data, discussing the results, and writing the manuscript.

Aggregate fragmentation is an important process for controlling the vertical flux of organic carbon in the ocean (Briggs et al. 2020). A variety of mesozooplankton groups has been found to feed on marine snow, including copepods, euphausiids, amphipods such as *Themisto*, nematodes, and polychaetes larvae (Alldredge 1972; Lampitt et al. 1993; Norrbin et al. 1996; Green and Dagg 1997; Kiørboe 2000; Cawley et al. 2021; Koski and Lombard 2022). The ingestion of sinking particles such as marine snow may occur through different feeding strategies and hence the impact of zooplankton on vertical flux attenuation is highly related to their feeding mode (Koski et al. 2017; Stukel et al. 2019). Most calanoid copepods are current-feeding, also referred to as suspension-feeding or filter-feeding (Kiørboe 2011) and may detect settling aggregates by hydromechanical signals (Visser and Jonsson 2000) or chemical trails (Kiørboe 2001). Current-feeding copepods may also break up larger particles like marine snow and fecal pellets into smaller and slower sinking objects, thus affecting vertical carbon flux indirectly (Iversen and Poulsen 2007; Svensen et al. 2012). Cruise-feeding copepods may search for marine snow to colonize and feed on (Kiørboe 2000), while ambush feeding copepods like *Oithona* spp. utilize hydromechanical signals to detect and feed on sinking or swimming prey particles (Svensen and Kiørboe 2000). A special case of ambush feeders are the flux feeders (Kiørboe 2011), described as organisms passively collecting sinking particles in mucus nets, such as Pteropods (Jackson 1993). For flux feeders, the feeding rate is proportional to the concentration of particles and their sinking velocity (Jackson 1993). Some copepod species, such as *Oncaea* spp., *Triconia* spp., and *Microsetella norvegica*, appear especially adapted to feed on aggregated food (Koski et al. 2020; Koski and Lombard 2022) and feed poorly on suspended particles (Koski et al. 2005, 2017), unless the concentration of suspended particles is high (Uye et al. 2002). Copepods with this specific behavior are referred to as particle- or aggregate-colonizing copepods. While suspension or ambush feeding copepods most often feed on marine snow particles in proportion to their availability, particle-colonizing copepods will actively search for aggregates (Kiørboe 2011). The importance of particle-colonizing copepods as degraders of marine snow will hence depend on the copepod abundance, while the effect of suspension-feeding calanoid copepods might thus mainly depend on the concentration of marine snow particles in relation to other food sources (Koski and Lombard 2022). Particle-colonizing copepods are therefore considered important for the carbon budgets of the surface oceans (Koski et al. 2020).

In a wide range of coastal ecosystems ranging from 34°N to 70°N, *M. norvegica* can occur at high densities, provided that they are sampled with, for example, small mesh-sized nets or water bottles (Arendt et al. 2013; Svensen et al. 2018). For example, *M. norvegica* may reach high densities of > 70,000 ind. m^{-3} in a variety of ecosystems such as Godhåpsfjord (Greenland), Porsangerfjorden (northern-Norway), and the Inland Sea of Japan (Uye et al. 2002; Arendt et al. 2013; Mooney et al. 2023). Hence, *M. norvegica* may outnumber calanoid copepods and other consumers of marine snow particles. Previous studies show that *M. norvegica* can cover its daily metabolic demands by feeding on a variety of aggregates, and most of the carbon is consumed in the upper 0–50 surface layer where the copepod is most abundant (Koski et al. 2020). Despite the general important role of zooplankton for regulating the biological pump, direct evidence of interactions between zooplankton and aggregates are rare (van der Jagt et al. 2020). This is also the case for *M. norvegica*. Although it has previously been observed associated with marine snow in situ (Green and Dagg 1997; Mooney et al. 2023) and ingestion rates have been quantified (Koski and Lombard 2022), few studies have done both simultaneously. In this study, we attempt to combine in situ observations of marine snow and *M. norvegica* with estimates of ingestion rates, measurements of the vertical carbon flux from sediment traps and a description of the behavior of *M. norvegica* in relation to sinking marine snow and fecal pellets. We hypothesized that (1) high concentrations of *M. norvegica* coincide with high carbon flux attenuation due to its colonization and feeding on sinking aggregates, and that (2) the importance of *M. norvegica* on the carbon flux attenuation is dependent on the aggregate type. By combining in situ observations and laboratory measurements, we aim to highlight the potential importance of a small-sized and under-sampled particle-colonizing copepod for carbon consumption and export in a high latitude coastal ecosystem.

Materials and methods

Site description

The study was conducted during 2 consecutive years in the sub-arctic Balsfjord (sill depth 55 m) on June 18–21, 2017 and June 11–14, 2018, at station Svartnes (69°21.8′N, 019°07.0′E, basin depth 180 m). Balsfjord is a productive cold-water fjord located above the polar circle, featuring arctic light conditions with midnight sun during summer (May–July) and polar night in winter (November–January). In winter the water column is cold (typically 1–3°C) and often vertically mixed. In summer the water column tends to be strongly stratified with warmer and fresher surface waters (Eilertsen and Taasen 1984; Eilertsen and Skardhamar 2006). Phytoplankton abundance is high in April (Eilertsen et al. 1981) and the primary production peaks in April (up to 1000 mg C m^{-2} d^{-1}) and remains high until August (around 200–400 mg C m^{-2} d^{-1}) (Eilertsen and Taasen 1984). The study site represents a high-latitude fjord with strong seasonal pulses of productivity and arctic features regarding temperature and light regime.

Sampling and analysis

Temperature, salinity, and fluorescence in the water column were measured with a conductivity, temperature, and depth probe (CTD, Seabird SBE911+) equipped with a fluorescence

sensor, at an approximate interval of 4 h, obtaining a total of 12 profiles during each of the two sampling campaigns.

Samples of water for chlorophyll *a* (Chl *a*), particulate organic carbon (POC) concentrations, community composition of planktonic protist (including autotrophic protist commonly named phytoplankton) and abundance of small metazoans were collected at 0, 10, 50, 90, and 120 m depth, using a 30-liter GoFlo water bottle (General Oceanics). Samples were collected twice during each field campaign, and the mean of these two values is presented. For total Chl *a* concentration, triplicate subsamples of 200 mL were filtered onto GF/F filters. In addition, one replicate of 300 mL was filtered onto a 10-μm Millipore filter for the concentration of Chl *a* in the $>10\,\mu$m particle size fraction. The filters were stored frozen (-20°C) for <1 month and then Chl *a* concentration was determined with Turner design fluorometer after 20 h extraction in 5 mL methanol and according to the acidification method (Holm-Hansen et al. 1965). For POC concentration, triplicates of 300–500 mL aliquots of the water sample were filtered onto pre-combusted GF/F filters. The filters were stored frozen (-20°C) until analyzed on an elemental analyzer (Lab Leeman 440 Elemental Analyzer), after fuming with concentrated HCl to remove inorganic carbon (calcium carbonate).

For analyses of the protist plankton composition, subsamples of 100 mL were collected from each depth. The samples were fixed with an acidic Lugol's solution to a final concentration of 2% and stored in dark bottles until laboratory analysis. Subsamples were analyzed according to the protocols described by Utermöhl (1958) and modified by Edler (1979). Protists were counted under an inverted microscope equipped with phase and interference contrasts (Nikon Eclipse TE-300). Microplankton ($>20\,\mu$m) was enumerated from the entire chamber surface at 100× magnification. Nanoplanktonic cells (3–20 μm) were counted at 400× magnification by moving the field of view along the length of three transverse transects. For the most numerous taxa, up to 50 specimens were counted. Systematic affiliation of the identified taxa was verified against the World Register of Marine Species (WoRMS). Except for the indeterminate flagellates (Flagellate indet.), other taxa were classified into one of the major units in the rank of class or phylum.

The remaining 20 liters of the GoFlo bottle was gently emptied via a silicone tube attached to the GoFlo outflow valve. The water sample was concentrated onto a 20-μm meshed sieve and transferred to a PVC bottle for later counts of *M. norvegica*. In addition, the zooplankton community was sampled with a WP-2 type net (Hydrobios Apparatebau GmbH) in two depth intervals (50–0 and 170–50 m). The net and its cod end had a mesh size of 64 μm and was used with a closing mechanism for stratified sampling. Due to the small mesh-size, the net was hauled vertically at low speed, 0.2–0.3 m s^{-1}. Five vertical profiles (at approximately 6-h intervals) were sampled in 2017 to quantify differences in vertical distributions over a 24-h cycle. In 2018, one profile for abundance was sampled during daytime, while the diel vertical distribution of zooplankton was determined using in situ optics (*see* below). On deck, the contents of the cod-ends were gently rinsed onto a 64-μm sieve and transferred to 100-mL PVC bottles. All zooplankton samples were preserved with sodium tetraborate buffered formaldehyde in filtered seawater at 4% final concentration.

Zooplankton samples were examined with an Olympus model SZX7 stereomicroscope according to the procedures described in Sameoto et al. (2000) and Kwasniewski et al. (2010). Additionally, copepodite life stages CI–CV of *M. norvegica* were identified at higher magnification using an Olympus light microscope model BX50. Zooplankton identification and enumeration was carried out on subsamples obtained from the entire sample by taking 2 mL aliquots from a known volume of the sample dispersed in a calibrated beaker. From each sample, at least 500 individuals were examined from 5 to 10 subsamples. The remainder of the sample was screened in its entirety for the presence of individuals of rare species. Half of the GoFlo samples were examined in their entirety, while for the other half and for a few of WP-2 net samples, splitting with a box splitter was required before subsampling due to extremely high zooplankton abundances. The smallest fraction analyzed in detail for GoFlo samples was 1/6 of the whole sample, and for the WP-2 net samples it was 1/120.

The population biomass of *M. norvegica* was estimated using stage-specific body length, empirical length-carbon correlation for individual stages (Uye et al. 2002), and data on the number of copepodid stages in the samples obtained in this study.

Under water imaging

In addition to net-tows and water bottle sampling, high-resolution images were obtained with an autonomous digital Video Plankton Recorder (VPR; Seascan Inc) to investigate the vertical abundance and distribution of *M. norvegica*, marine snow and fecal pellets at higher temporal and spatial resolution. The VPR was equipped with a Unix 1.4 megapixel black and white camera, a synchronized Xenon strobe, and additional hydrographic sensors including a Seabird SB49 Fastcat CTD and a WetLabs Ecopuck fluorescence/turbidity sensor. We used a camera setting with a magnification best suitable for the abundant mesozooplankton species (e.g., copepods), and a 22×32.5 mm field of view, resulting in a calibrated image volume of 35.2 mL per frame and a pixel resolution of 24.3 μm.

The instrument was undulated between surface and bottom from a ship at anchor with a vertical velocity of ca 0.8 m s^{-1}, sampling on average 20 images s^{-1}. The compressed data were uploaded to a computer for analysis beginning with extraction of regions of interest (ROIs) using the Autodeck program (Seascan Inc.). Postprocessing was done using the Visual Plankton package (CS Davis, Woods Hole Oceanographic Institution) and own Matlab (Marth Works) scripts (F. Norrbin) to obtain

vertical concentrations and size-distributions of particles. For selected profiles, full manual analyses of the entire frames were made (4000–5000 image frames in each depth profile), revealing detailed distribution of *M. norvegica*, marine snow, fecal pellets, and copepods attached to fecal pellets.

In 2017, we made five VPR casts, each comprising three to five "tow-yos" (down and up vertical profiles), at different times of the day and night. In 2018, we sampled continuously for 24 h, pausing only to download data and change the batteries. The volume sampled for each vertical profile was approximately 150 liters and the total volume for each "tow-yo" is thus 300 liters.

VPR imaging data from both years were used to obtain an index of fine-scale vertical abundance and distribution of *M. norvegica* individuals, marine snow, fecal pellets and *M. norvegica* attached to FP. Hourly weighted mean depths (WMD) is a common measure of the center of gravity of vertical distribution patterns to observe overall changes in vertical depth distribution over the whole water column and were computed for each VPR deployment as: $\mathrm{WMD} = (\sum n_i\, d_i / \sum n_i)$, where n_i is the respective abundance (ind.$^{-1}$ L) in depth stratum I (stratum thickness 1 m) with midpoint depth d_i (Frost and Franzen 1992).

Downward flux of carbon and particles

The downward flux of sinking material was measured at 20, 30, 50, 90, and 120 m, using short-term sediment traps (KC Denmark). The traps consisted of two to four plexiglass cylinders, each with a volume of 1.8 liters and aspect ratio 6.25, mounted in a steel frame attached to a mooring. The mooring was anchored to the sea floor, and the deployment time was 22–24 h. For cylindrical traps, an aspect ratio above 5 is likely to ensure good collection efficiency (Buesseler et al. 2007). The catch-efficiency of sediment traps similar to those applied here has previously been evaluated as comparable with estimates of downward carbon flux obtained with the ^{234}Th method (Coppola et al. 2002) and neutrally buoyant sediment traps (Baker et al. 2020).

One 24-h deployment was conducted in 2017, and five deployments were conducted in 2018. After recovery of the mooring, the content of the cylinders from each deployment depth was gently pooled, and subsamples were taken for analyses of the Chl *a* and POC flux and the composition of sinking protist plankton. The samples were treated and analyzed as described for the water column samples. Swimmers were as far as possible removed from the filters after filtration of the sediment trap material. To compare the relative reduction of carbon in the surface in 2017 and 2018, the fractional loss rates of carbon flux (F) between 20 and 50 m were calculated as $1 - F_{50}/F_{20}$, where F_{50} and F_{20} is the carbon flux (mg C m^{-2} d^{-1}) measured at 50 and 20 m, respectively (van der Jagt et al. 2020).

Sinking velocity (SV, m d^{-1}) of marine snow aggregates ($n = 13$) were measured individually in the laboratory using the same set-up as described below for *M. norvegica* behavior, while sinking velocity for krill pellets were calculated from the mean pellet size obtained in situ (0–170 m depth) and the regression by Stukel et al. (2019).

Measuring of feeding rates and observations of *Microsetella* behavior

Feeding rate of *M. norvegica* on aggregates was estimated based on the functional response of pellet production of adults or copepodids CV to increasing concentrations of aggregates, using algal aggregates (marine snow) in 2017 and intact and aggregated fecal pellets of krill in 2018. Aggregates for the incubations were collected from the sediment traps. The aggregate concentrations ranged from 0 to 16 aggregates per bottle, with 5–6 concentrations and 2–3 replicate experiments per aggregate concentration and type. All *M. norvegica* individuals were starved for a minimum of 12 h before the experiments, by incubating them in 0.5-liter airtight closed tissue flasks containing 0.2 μm filtered seawater, at the experimental temperature of 8°C. After starvation stage, 10–20 *M. norvegica* individuals were placed into 70-mL tissue flasks containing filtered seawater and target concentrations of aggregates. The incubation bottles were closed airtight and placed in a plankton wheel, turning at the speed of one round per minute. After approximately 24 h, the contents of the bottles were carefully poured into Petri-dishes, *M. norvegica* individuals and pellets were counted using a Zeiss Discovery V12 stereoscope, and the Petri-dishes were photographed using a Zeiss axiocam for later measurements of pellet and aggregate sizes.

All marine snow aggregates that were incubated in the grazing experiments were imaged prior to the incubations and their area was determined using ImageJ. First their area (A, μm^2) was converted to diameter (D, μm). Thereafter, the diameter was used to calculate the volume (V_{ms}, μm^3) of each aggregate, assuming spherical shape. To determine the krill fecal pellets, we used the measure of pellet length (L, μm) and diameter (D_{fp}, μm) to determine their volumes (V_{fp}, μm^3), assuming cylindrical shape. To convert the marine snow and krill fecal pellet volume to particulate organic carbon ($\mathrm{POC}_{\mathrm{ms}}$, mg) content, we filtered several marine snow aggregates or fecal pellets of similar volume onto individual combusted GF/F filters and measured the total POC content. This was done for three different size-classes: small (0.5–1 mm), medium (1–2 mm), and large aggregates (2–3 mm). From this, we obtained size specific POC content of the aggregates and used the following regression to calculate the POC content of each aggregate added to each treatment of the grazing incubations:

$$\mathrm{POC}_{\mathrm{ms}} = 0.1852 \times {V_{\mathrm{ms}}}^{0.4799} \quad (1)$$

For the krill fecal pellets, individual length and width were measured and the volume was converted to POC using the conversion factor (0.036 mg POC mm^{-3}) from Belcher et al. (2016). To get the total added POC per treatment, we summed

the POC content of all marine snow aggregates or all krill fecal pellets that were added to each treatment.

The *M. norvegica* ingestion rate on aggregates was estimated based on the pellet production. First, the average carbon content of *M. norvegica* pellets was estimated by measuring the lengths and widths of approximately 60 pellets from incubations using *Thalassiosira weissflogii* as food. Their volume was estimated by assuming an ellipsoidal shape, and the volume was converted to carbon using the volume to carbon conversions of Reigstad et al. (2005). This pellet carbon content of $0.012 \pm 0.013\ \mu$g C pellet^{-1} was multiplied with the pellet production in each incubation, and converted to ingestion assuming 30% assimilation efficiency, as measured by Ploug et al. (2008) for the copepod *Temora longicornis* feeding on *T. weissflogii*. The estimated ingestion rates were plotted as a function of aggregate concentration (all in carbon) and fitted with a hyperbolic function ($y = ax/b + x$) to obtain the coefficients a and b. Search volume (β), handling time (τ), and maximum ingestion rate (i_{max}) were estimated based on the Holling type II functional response (Holling 1966), according to

$$i = \beta C_{agg} / \left(1 + \beta \tau C_{agg}\right), \quad (2)$$

where i is the ingestion rate (in μg C ind.$^{-1}$ d^{-1}), β is the search volume (L ind.$^{-1}$d^{-1}), τ is the handling time (in days), and C_{agg} is the aggregate concentration (in μg C L^{-1}). The maximum ingestion rate (i_{max}) was assumed to be the inverse of the handling time, and β and τ were calculated based on the coefficients so that $\beta = a/b$ and $\tau = 1/b$. Weight-specific ingestion rates were based on individual length- and carbon-measurements of *M. norvegica* females as described in Barth-Jensen et al. (2020). The mean size of *M. norvegica* females was $478 \pm 22\ \mu$m and the mean carbon weight was $0.42\ \mu$g C ind.$^{-1}$.

To investigate swimming behavior in presence and absence of marine snow, female *M. norvegica* were placed in a plexiglass aquarium ($5 \times 5 \times 20$ cm, width, depth, and height) in a temperature-controlled lab at 8°C. The aquarium was filled with GF/F filtered seawater and *M. norvegica* were observed in the absence or in the presence of marine snow aggregates. Individual copepods were followed between 1 and 5 min in each treatment until a total of 30 min with copepods in focus was obtained. For the swimming behavior in the presence of marine snow, individual marine snow aggregates were allowed to sink through the aquarium while the copepods were observed (kept in focus with the camera). The camera system consisted of a Basler acA1300-30gc camera (1 Mega-pixel with its infrared filter removed) equipped with a Sigma 105-mm macro lens (EX Sigma, 105 mm 1 : 2-8D, DG Marcro). The illumination was done from the back with an infrared backlight (MBJ DBL plate, 880 nm). In total, ~ 30 min of swimming behavior was analyzed for each treatment by following 10 individual copepods in filtered seawater and 12 copepods in the aggregate treatment. The feeding bout frequency was calculated as numbers of leg flicks during the duration of each sinking event. The swimming behavior was analyzed as total duration spent sinking and swimming, and swimming and sinking velocities. Total distances of sinking and swimming were calculated, and the number of feeding bouts were counted per sinking event and calculated as frequency of feeding bouts during sinking by dividing the number of feeding bouts with the duration of sinking for each event. The behavior of female *M. norvegica* in filtered seawater and in water with particles were tested for statistical differences using a student's *t*-test.

Results

Marine snow, fecal pellets, and downward flux of particulate organic matter

The 2-yr investigation differed in terms of dominating particle type and concentrations as well as depth distributions of marine snow and fecal pellets (Table 1). In 2018, marine snow concentrations were negligible. In contrast, high mean surface concentrations of 4.92 ± 4.48 marine snow aggregates L^{-1} were observed in the upper 50 m in 2017. Below 50 m, the marine snow abundance decreased abruptly to less than 0.1 L^{-1}. The mean spherical diameter (ESD) of the marine snow was higher in the surface (2.73 ± 1.24 mm) than below 50 m (1.77 ± 0.74 mm ESD) in 2017. Diatom chains and detritus were visible components of the marine snow in 2017 (Fig. 1; Supplementary Fig. S1).

In 2018, the few marine snow particles observed were smaller than in 2017, with ESD ranging from 1.37 ± 0.74 in the surface 50 m to 1.08 ± 0.51 below 100 m (Table 1). Fecal pellets were abundant in 2018 with mean concentrations increasing from 0.69 ± 0.54 L^{-1} at 0–50 m to 1.76 ± 0.53 L^{-1} at 100–170 m. In 2017, the concentration of fecal pellets was considerably lower, 0.03 ± 0.03 L^{-1} in the upper 50 m and 0.42 ± 0.18 L^{-1} below 100 m (Table 1). The mean sinking velocity of krill fecal pellets (mean ESD 1.05 ± 0.54) was 447 ± 189 m d^{-1}, while the mean sinking velocity of marine snow was 98.2 ± 63.5 m d^{-1} (Supplementary Table S1). The sinking velocity of marine snow ($n = 13$) ranged from 29 to 216 m d^{-1} and was positively correlated with size ($R^2 = 0.56$) (data not shown). The weighted mean depth distribution of marine snow in 2017 was at 25.8 ± 2.9 m (Supplementary Table S2) and there was no apparent diurnal variation. In both years, fecal pellets were most abundant below 100 m, with the weighted mean depth of 124 ± 20.5 m in 2017 and 104.5 ± 13.0 m in 2018 (Supplementary Table S2).The fecal pellets in 2018 had distinctly uneven vertical distribution that seemed to follow a diel pattern; pellets were found in the surface waters at night between 22:00 and 02:00 h, and deeper during daytime (Supplementary Fig. S2), resulting in a wide depth range of WMD values in 2018. According to the VPR images, it is likely that a large fraction of the fecal pellets was produced by Euphausiids (Fig. 1d–f). The vertical distribution of fecal pellets likely reflected the feeding and production of pellets by Euphausiids in

Table 1. Size (mean ESD ± SD, mm) and abundance (# L^{-1}) of marine snow and fecal pellets in 0–50, 50–100, and 100–170 m depth intervals in 2017 and 2018. All values are calculated from the Video Plankton Recorder.

Year	Depth	0–50 m	50–100 m	100–170 m
2017	Marine snow, size	2.73 ± 1.24 (n = 9381)	1.77 ± 0.74 (n = 95)	1.82 ± 0.84 (n = 148)
	Marine snow, abundance	4.92 ± 4.48	0.08 ± 0.05	0.1 ± 0.06
	Fecal pellet, size	1.69 ± 0.81 (n = 815)	1.26 ± 0.60 (n = 790)	1.40 ± 0.65 (n = 1477)
	Fecal pellet, abundance	0.03 ± 0.03	0.31 ± 0.14	0.42 ± 0.18
2018	Marine snow, size	1.37 ± 0.74 (n = 404)	1.35 ± 0.72 (n = 182)	1.08 ± 0.51 (n = 738)
	Marine snow, abundance	0.01 ± 0.03	0.00 ± 0.00	0.03 ± 0.08
	Fecal pellet, size	1.10 ± 0.60 (n = 310)	1.08 ± 0.56 (n = 475)	0.99 ± 0.48 (n = 738)
	Fecal pellet, abundance	0.69 ± 0.54	1.29 ± 0.40	1.76 ± 0.53

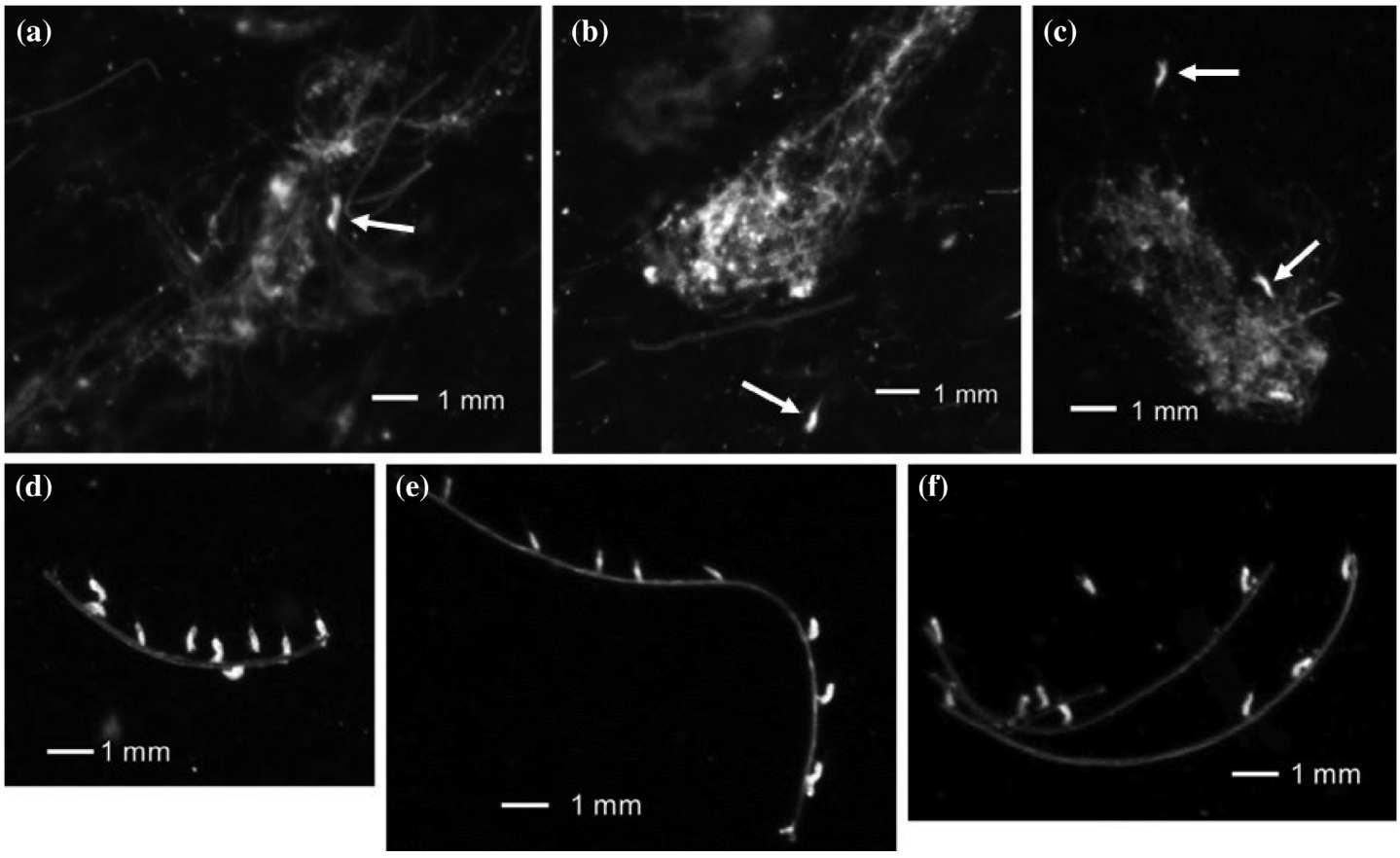

Fig. 1. In situ images obtained with the video plankton recorder showing *Microsetella norvegica* (depicted with white arrows) and marine snow particles in 2017 (**a**–**c**) and attached to fecal strings in 2018 (**c**–**f**).

the surface layer at night, with pellets sinking to deeper waters during the early morning and the day (Supplementary Fig. S2).

The quality and quantity of the downward carbon flux differed in the 2 yr of observation (Fig. 2). In 2017, the downward carbon flux at 20 m was 420 mg C m^{-2} d^{-1} and decreased with increasing depth. At 20 and 30 m, the export flux of Chl *a* was 3.5 mg m^{-2} d^{-1} and in terms of phytoplankton composition the main contributors were diatoms (Fig. 2).

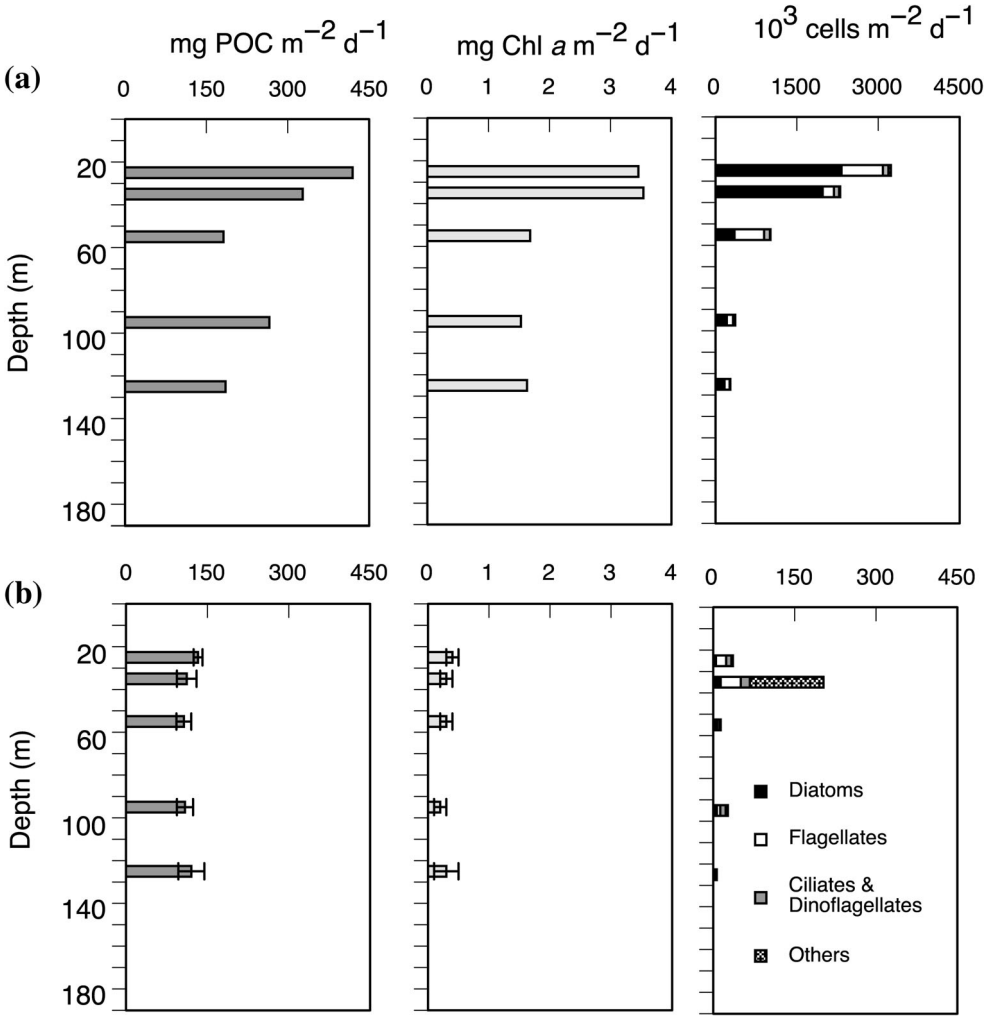

Fig. 2. Vertical flux of particulate organic carbon (mg POC m^{-2} d^{-1}), chlorophyll *a* (mg Chl *a* m^{-2} d^{-1}), and phytoplankton cells (10^3 cells m^{-2} d^{-1}) in 2017 (**a**) and 2018 (**b**). In 2018, the vertical flux of POC and Chl *a* is presented as mean ± SD of 5 consecutive sediment trap deployments. Note different scales on *x*-axes for phytoplankton cells.

In 2018, the downward flux at 20 m was 133 mg C m^{-2} d^{-1}, and thus much lower than in 2017.

The carbon flux was relatively constant with increasing depth and phytoplankton cells did not make a large contribution to the carbon flux (Fig. 2). The fractional loss rate of POC between 20 and 50 m depth was 0.57 in 2017 and 0.2 in 2018, which translated into a reduction of 238 and 26 mg C m^{-2} d^{-1}, respectively.

Physical and biological environment and copepod community

The differences in downward carbon flux in 2017 and 2018 reflected different seasonal development of hydrographic conditions and suspended biomass accumulation. Both sampling years had a stratified water column in June. However, the water was colder during the study period in 2018 than in 2017 (Fig. 3). The salinity at 0–50 m was lower in 2018 (32.8 ± 0.2) than in 2017 (33.1 ± 0.2) but at > 50 m it was somewhat higher in 2018 (33.5 ± 0.1) than in 2017 (33.3 ± 0.0). Concentrations of Chl *a*, phytoplankton cells (phototrophic protists), and POC in the water column were highest in the upper 20 m, but there were also some differences between the 2 yr (Supplementary Fig. S3). In 2017, the integrated concentrations (0–50 m) of total Chl *a* and POC were 104 and 13,000 mg m^{-2}, respectively. In contrast, concentrations in 2018 were only 29 mg Chl *a* m^{-2} and 6600 mg POC m^{-2} (data not shown). Diatoms dominated the phytoplankton community in 2017, mostly represented by the genera *Thalassiosira* and *Chaetoceros* whereas small, flagellated cells dominated the phytoplankton community in 2018 (Supplementary Fig. S3).

The population size of *M. norvegica* was generally large, with an exceptionally high abundance of almost 50 ind. L^{-1} in the surface layer in 2017 (Fig. 3). No apparent shift in

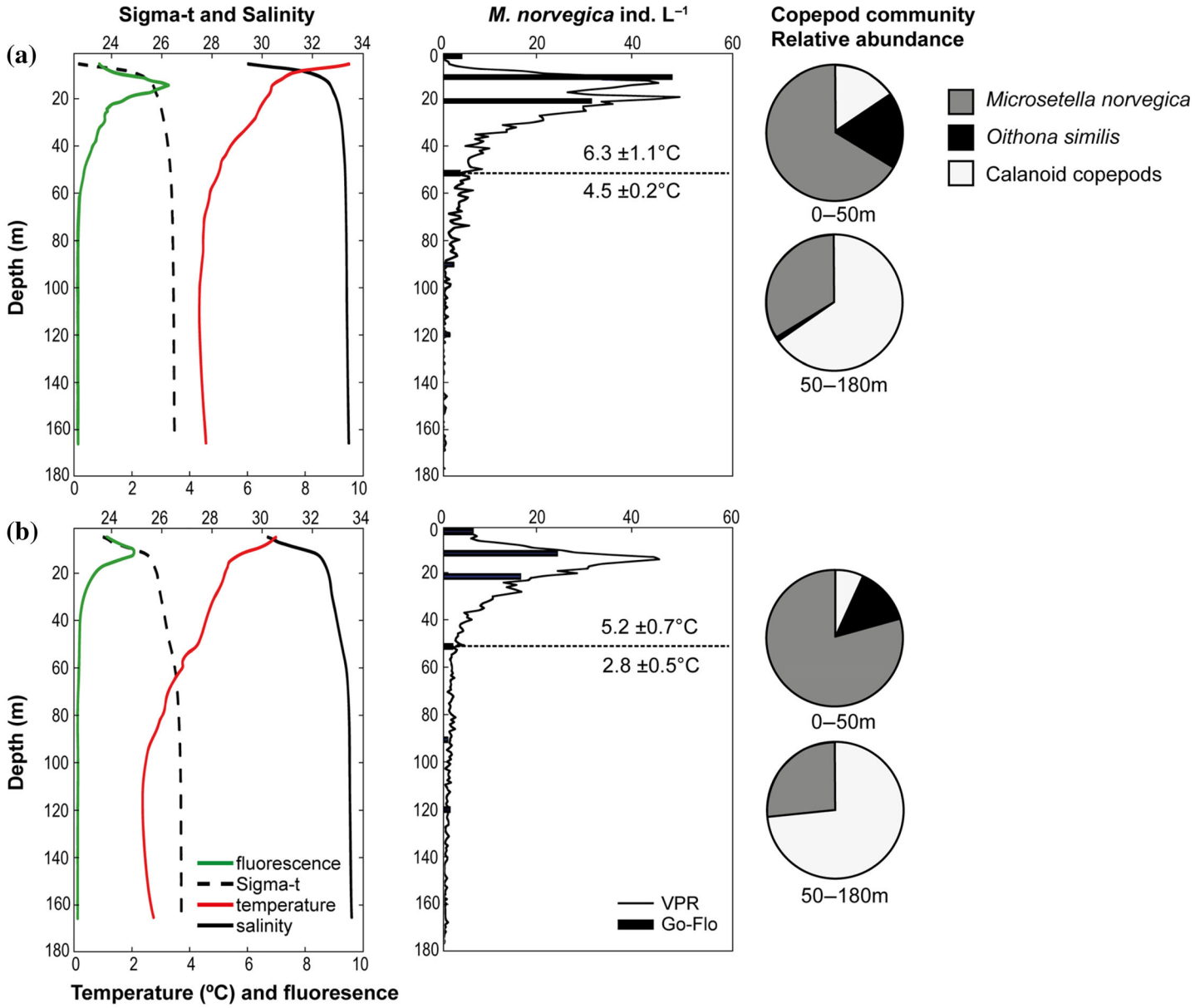

Fig. 3. Sigma-t, salinity, temperature (°C), and fluorescence in 2017 (**a**, left panel) and 2018 (**b**, left panel). Temperature (red lines) and salinity (black lines) are presented as mean values for 12 CTD profiles from each year. The middle panels show vertical distribution (ind. L^{-1}) of *Microsetella norvegica* obtained with the VPR and Go-Flo bottles. The black dotted line displays the temperature mean ± SD from 0 to 50 m (value above dotted line) and from 50 to 180 m (below dotted line) in 2017 (**a**) and 2018 (**b**). The right panels show relative composition of the copepod community in 2017 (**a**) and 2018 (**b**), as obtained with the WP-2 net sampling. CTD, conductivity, temperature, and depth; VPR, Video Plankton Recorder.

vertical distributions were detected over the 24-h cycle (Supplementary Fig. S4). The total integrated population biomass above the sediment traps (0–120 m) in 2017 and 2018 was 722 and 393 mg C m^{-2}, respectively (Table 2). Integrated over the entire water column, *M. norvegica* was by far the most abundant copepod species, followed by *Oithona similis* (Fig. 3). In the upper 50 m, *M. norvegica* contributed on average 63% of the total copepod abundance in 2017, and 81% in 2018 (Fig. 3). Calanoid copepods, mostly represented by *Calanus finmarchicus* and *Pseudocalanus* spp., were most abundant below 50 m. Abundances of *M. norvegica* obtained with the Go-Flo bottle and the VPR both showed maximum abundance of 20–40 ind. L^{-1} at 10–20 m depth (Fig. 3; Supplementary Fig. S4). However, copepod abundances obtained with the 64-μm meshed WP-2 net were generally 2–5 times lower compared to the Go-Flo and VPR (data not shown). We suggest that the WP-2 net under-estimated the abundance of *M. norvegica*, possibly due to clogging of the net by organic

Table 2. Integrated abundance (ind. m^{-2}), biomass (mg C m^{-2}) and potential carbon consumption (mg C m^{-2} d^{-1}) on marine snow in 2017 and intact krill pellets (FP_{int}) and aggregates of pellets (FP_{agg}) for the *Microsetella norvegica* population in the surface (0–50 m) and the deep (50–120 m) water layer. The *M. norvegica* abundance and biomass are calculated as the mean from two vertical GoFlo profiles for each year. The carbon consumption rates are obtained from integrated abundances and individual ingestion rates from the incubations.

Year	Depth interval (m)	Abundance (ind. m^{-2})	Biomass (mg C m^{-2})	Potential carbon consumption (mg C m^{-2} d^{-1})
2017	0–50	1,177,949	644	235
	50–120	207,900	78	42
2018	0–50	629,000	350	69 (FP_{int}), 214 (FP_{agg})
	50–120	147,800	43	16 (FP_{int}), 50 (FP_{agg})

particles in the water column. The data obtained with the WP-2 net are therefore only used for comparing the relative contribution of *M. norvegica* to the copepod community (Fig. 3). It should be noted that the abundance of krill could not be quantified with the methods applied in this study, and therefore their grazing and fecal pellet production rate are not addressed.

Interaction between *Microsetella* and particles

In 2018, *M. norvegica* were observed attached to krill pellets (Fig. 1d–f), and this phenomenon was registered at a weighted mean depth of 82.4 ± 34.4 m (Supplementary Table S2). In 2017, *M. norvegica* were most abundant at 20–30 m, in the same depth-range as marine snow (Supplementary Table S2), but no attachments were directly observed (Fig. 1a–c). In the laboratory experiments, *M. norvegica* was actively feeding both on algal aggregates and on krill fecal pellets, indicated by fecal pellet production rates that increased from < 1 pellet ind.$^{-1}$ d^{-1} in the incubations with the lowest aggregate concentrations to up to 6 pellets ind.$^{-1}$ d^{-1} in the incubations at saturating concentrations (Fig. 4). However, a shorter handling time and a higher maximum ingestion rate on algal aggregates and aggregated fecal pellets than on intact fecal pellets (Supplementary Table S3) suggest that it was easier for *M. norvegica* to obtain food from algal aggregates than from intact krill pellets.

The calculated feeding rates ranged approximately sevenfold, depending on the aggregate concentration and type (Supplementary Table S3). Ingestion rates of *M. norvegica* was 0.20 μg C ind.$^{-1}$ d^{-1} on algal aggregates, 0.11 μg C ind.$^{-1}$ d^{-1} on intact krill pellets and 0.34 μg C ind.$^{-1}$ d^{-1} on aggregated fecal pellets. With a measured female carbon weight of 0.42 μg ind.$^{-1}$ (Barth-Jensen et al. 2020), the ingestion rates correspond to 48% body carbon d^{-1} and 26–80% body carbon d^{-1} for algal aggregates and krill fecal pellets, respectively.

The swimming velocity of *M. norvegica* in filtered seawater and with marine snow was 1.1 and 1.3 mm s^{-1}, respectively (Supplementary Table S3; Supplementary Video S1). When *M. norvegica* were incubated in filtered seawater without the addition of aggregates, the copepod had active upward swimming periods of 45 ± 33 s, followed by a period of passive sinking for 65 ± 43 s. When incubated in filtered seawater with added marine snow aggregates, the time spent swimming was 79 ± 80 s followed by a period of passive sinking of 64 ± 25 s. Thus, the swimming period appeared longer when food particles were present in the surrounding water, but this

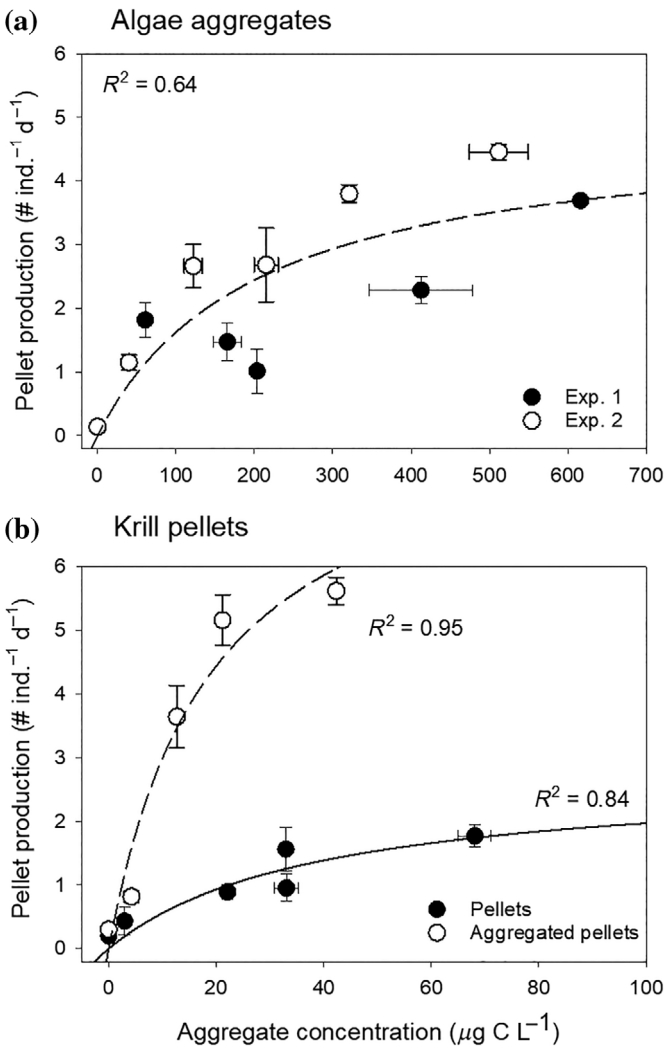

Fig. 4. *Microsetella norvegica* pellet production (pellets ind.$^{-1}$ d^{-1}) as a function of aggregate concentration (μg C L^{-1}) on (**a**) algae aggregates (2017) and (**b**) single or aggregated (decaying) krill fecal pellets (2018; mean ± SE). Different symbols indicate different experiments. The lines indicate the Holling II type functional response (hyperbola); R^2 of each equation is given in the figure.

was not statistically significant (Student's t-test: $p = 0.231$). While *M. norvegica* only swam upward when incubated in filtered seawater without marine snow, they swam horizontally when encountering marine snow or marine snow fragments (Supplementary Video S2). The main difference in swimming behavior between the incubations with and without marine snow was observed for the feeding bout frequency during sinking events (Supplementary Table S3), which was significantly higher in the presence of marine snow compared to when the copepods were only incubated in filtered seawater (Student's t-test: $p = 0.0152$).

Discussion

Carbon export flux

The downward flux of carbon was higher in 2017 than in 2018, reflecting different phytoplankton communities. However, the grazer community in 2017 and 2018 was not different in terms of abundances and species composition. The most abundant copepod in the surface was *M. norvegica*, while other important grazers such as *C. finmarchicus* were found mostly below 50 m depth. Despite the comparable copepod communities in 2017 and 2018, a strong reduction of carbon flux with depth was only apparent in 2017. We suggest that this was mainly due to differences in the phytoplankton community and suspended biomass in the 2 years, combined with feeding preferences and potential impact of the most abundant copepod species, *M. norvegica*.

Microsetella feeding, swimming behavior, and impact on sinking flux

Feeding

Our results demonstrated that *M. norvegica* can feed both on algal aggregates and fecal pellets, although the feeding rates on algal aggregates and aggregated (likely decaying) fecal pellets were twice as high as the feeding rates on intact fecal pellets. These rates were within the range of previous measurements (Koski and Lombard 2022) and confirmed that the aggregate quality influences the feeding rates. The aggregate quality can both influence the encounter rate (the slope of the functional response) and the handling time (the saturation) where the encounter rate describes the efficiency by which *M. norvegica* can find the aggregates and the handling time describes the efficiency by which *M. norvegica* can extract nutrition from the encountered aggregate. The encounter rate is in general influenced by the aggregate size, the chemical trail that it might leave in its wake and its sinking rate in relation to the swimming velocity of the copepod (Lombard et al. 2013), whereas the handling time could be a result of the nutritional quality of the aggregate, for example, through a higher assimilation efficiency of algal aggregates. In the current experiments, *M. norvegica* encounter rate was several-folds higher on fecal pellets than on algal aggregates despite the smaller size of the pellets, suggesting that factors other than size were important. For instance, it is conceivable that algal aggregates and aggregated fecal pellets leak more chemical substances (e.g., amino acids) than fresh pellets with intact membranes, although in our experiments this could only explain the difference between the two pellet types. However, size of the aggregate might become more important when aggregate concentrations are lower. For instance, the pellet production rate of a semi-benthic harpacticoid *Amonardia normanni* was related to the aggregate size in incubations with only one aggregate, whereas the size was not important in incubations with multiple aggregates (Koski and Lombard 2022), similar to the setup of the present study.

The handling time of intact pellets was long and the maximum ingestion rate thus lower than that of algal aggregates or aggregated pellets. This could either reflect the effect of a membrane that could both reduce the attachment and the ability of *M. norvegica* to extract nutrition from the aggregate or a lower nutritional quality of a pellet. Although we do not know the nutritional quality of pellets vs. algal aggregates, the lower nutritional quality of fecal pellets is supported by observations on bacterial growth, which was considerably higher on aggregates consisting of algae than on fecal pellets (Simon et al. 1990), and by the typically high C : N ratios of fecal pellets (Tamelander et al. 2012). Due to low nutritional quality, it seems likely that fecal pellets will be consumed at a lower rate than algal aggregates, at rates that are close to the ingestion rates on newly produced appendicularian houses (Koski and Lombard 2022).

The estimated maximum ingestion rates of *M. norvegica* on algal aggregates and aggregated fecal pellets, up to 80% body carbon d^{-1}, were within the ranges observed for copepods feeding on diatoms and microzooplankton. For instance, Dutz et al. (2008) demonstrated weight-specific ingestion rates of *T. longicornis* of > 100% body weight d^{-1} on diverse diatom diets. The only existing previous estimate of the in situ feeding rate of *M. norvegica* suggested 0.43 μg C $ind.^{-1}$ d^{-1} based on gut chlorophyll or 0.24 μg C $ind.^{-1}$ d^{-1} based on respiration rate, corresponding to ca. 50–100% body weight d^{-1} (Koski et al. 2020). The feeding rates obtained in the present study thus appeared realistic and comparable to previous observations.

Swimming behavior

Microsetella norvegica were more active in the presence of marine snow than in filtered seawater, swimming in a way that is typical for copepods that use chemical trails to detect settling aggregates (Kiørboe 2001; Lombard et al. 2013). *Microsetella norvegica* presented short feeding bursts while sinking, suggesting that it "tasted" the water while sinking. These observations propose that *M. norvegica* can actively change their swimming behavior from a vertical to a horizontal search pattern with frequent tasting or testing of the water to detect food particles. When a marine snow particle is encountered by a particle-feeding copepod, the predicted behavior is to fill the gut and leave the aggregate within minutes (Kiørboe 2000).

However, the measured handling times were long, suggesting that the copepods remained in the aggregates that they had once encountered, similar to previous observations (Koski et al. 2007). It is unknown why we did not observe *M. norvegica* on algal aggregates in 2017, although *M. norvegica* in 2018 was observed attached to krill pellets. Most of the pellets with *M. norvegica* attached were found at ca 80 m depth, while the weighted mean depth of pellets without *M. norvegica* was at 104 m. This may indicate that some copepods attach to pellets in the shallow water column, possibly to feed, whereby they are carried to the deeper part of the fjord with rapidly sinking fecal pellets. Possibly, the long handling time of pellets could explain why *M. norvegica* was still attached to pellets at depth, although the mechanisms behind copepod–aggregate interactions are not fully understood.

Effect on vertical flux

Coherent with the observed active search behavior of *M. norvegica*, the in situ abundance and size of marine snow particles decreased abruptly below 50 m depth in 2017. During the investigated period, the estimated total carbon consumption of the *M. norvegica* population in the upper 50 m depth (235 mg C m^{-2} d^{-1}) compared well with the measured decrease in carbon flux between 20 and 50 m (238 mg C m^{-2} d^{-1}). According to these calculations, *M. norvegica* could be responsible for the entire attenuation of the downward carbon flux in 2017. In contrast, the in situ abundance of fecal pellets increased with increasing depth in 2018. This suggests that either the pellets were not grazed upon by *M. norvegica*, or that pellets accumulated with depth or were produced deeper than 50 m. The Krill population in Balsfjord is dominated by the largely herbivorous species *Thysanoessa raschii* and *Thysanoessa inermis* that are known to perform diel vertical migration during summer (Falk-Petersen and Hopkins 1981). The sinking rate of krill fecal pellets in this study was estimated to 447 ± 189 m d^{-1}, implying a residence time of less than 3 h in the upper 50 m where most of the *M. norvegica* population was located. In comparison, the mean sinking velocity of marine snow was 98 ± 63 m d^{-1}, suggesting a residence time in the upper 50 m of 12.5 h or longer for the smaller marine snow particles. We suggest that the krill pellets were sinking too fast to allow *M. norvegica* grazing on such a scale that would have an impact on the vertical flux attenuation in 2018. While the ingestion rates on decaying aggregates of pellets were about three times higher than on intact pellets, it is difficult to transfer these rates to in situ conditions since this type of aggregates were not identified with the VPR and abundances in the water column could not be quantified.

It should be emphasized that the estimated impact of *M. norvegica* on downward carbon flux attenuation is associated with uncertainties. First, the estimations of carbon consumption depend on reliable measurements of individual ingestion rates on various food items that are also relevant for in situ conditions. In this study, ingestion rates were obtained by bottle incubations but the food particles were collected from sediment traps, which links the laboratory measurements to the field. The method of inferring ingestion rates from functional responses has also previously been successfully applied for the species (e.g., Koski et al. 2020). Second, the estimates of carbon consumption rely on accurate abundances and biomass of *M. norvegica*, which were obtained independently from water bottles, a plankton net with small mesh-size and VPR. This approach ensures robust data on *M. norvegica* abundances in the water column. Methods for measurements of downward carbon fluxes are also a matter of debate, and different types of sediment traps have their own advantages and disadvantages (Baker et al. 2020). The choice of non-drifting short-term sediment traps as used in the present study was based on the advantage of sampling multiple depths simultaneously, a recommended aspect ratio > 5 (Buesseler et al. 2007) and the geographical location of the study (a fjord system). Despite unavoidable uncertainties, we think that the impact of *M. norvegica* on downward carbon flux attenuation may be significant in specific conditions when the abundance of *M. norvegica* is high, and when slow-sinking marine snow is formed in the surface. However, the impact appears to be insignificant when the downward flux is dominated by large, fast-sinking, and intact fecal pellets and when the abundance of *M. norvegica* is low. In other words, in areas where *M. norvegica* is abundant, small and slow-sinking particles are more likely to be degraded in the upper water column while large, fast-sinking particles such as intact krill fecal pellets are most likely to avoid being grazed.

Small copepods and carbon attenuation

For a long time, *M. norvegica* and other small copepods have been overlooked since they are not sampled by the mesh-sizes of traditionally used plankton nets (Turner 2004; Svensen et al. 2011, 2018). The ecological role of small copepods has thus largely been ignored, although they are more recently suggested to have an important impact on flux attenuation (Kiørboe 2000; Koski et al. 2005, 2020). To date, their role for flux attenuation has only once been included in ecosystem modeling, and it was suggested that small copepods primarily attenuated the carbon flux via fragmentation of settling aggregates (Mayor et al. 2020). However, as Mayor et al. (2020) state, their model representation of the small copepods is speculative due to limited understanding of the physiology and ecology of these organisms. Their assumptions of small copepods having an ambush feeding mode, and thus low feeding rates and a feeding strategy of long motionless periods interrupted by jumps to intercept settling aggregates in their vicinity, seems to fit for small cyclopoid copepods such as *Oithona* spp. and *Triconia* spp. (Svensen and Kiørboe 2000; Iversen and Poulsen 2007; Koski and Lombard 2022). However, based on our observations and those of Koski et al. (2020), we argue that the harpacticoid copepod *M. norvegica*

has a more active lifestyle and higher feeding rates than the typical ambush feeding copepod.

Microsetella norvegica is typically found at shallow depths, which may be due to the active lifestyle and the general upward swimming patterns in searching for food. Small-sized aggregates are typically observed at shallower depths immediately below the Chl *a* maximum (Iversen et al. 2010), where they can readily be consumed by *M. norvegica*. The lower feeding rates on fast-settling aggregates the high pigment content in the guts of *M. norvegica* (Koski et al. 2020) suggest that *M. norvegica* primarily feed on freshly formed slow-settling phytoplankton aggregates. Typical abundances of *M. norvegica* are between 10^4 and 10^5 individuals m^{-3} (Dugas and Koslow 1984; Uye et al. 2002; Arendt et al. 2013; Svensen et al. 2018). Using our feeding rates, this is equivalent to a total aggregate ingestion of up to 1–34 mg C m^{-3} d^{-1} during periods with high aggregate concentrations. In deep-water oceans, less than 3% of the net primary production reaches the ocean floor (Iversen 2023). The typical downward carbon flux in the North Atlantic open ocean is decreasing by 40–50 mg C m^{-2} d^{-1} between 50 and 100 m (Iversen et al. 2010; Marsay et al. 2015) and zooplankton have been recognized as gatekeepers for the particulate carbon export below the euphotic zone (Jackson and Checkley 2011). Downward carbon flux attenuation appears strongly affected by the feeding behavior and ingestion rates of the zooplankton community combined with the type and sinking velocity of the particle, suggesting that small copepods are efficient gatekeepers, responsible for a substantially carbon turn over in the upper water column. It appears that even thin layers of particle-colonizing copepods may contribute substantially to the overall flux attenuation.

Even though different species of small copepods may have similar dietary preferences, they may diverge in other aspects. For example, the vertical distribution and population dynamics of *M. norvegica* and *Triconia* spp. are different. For instance, whereas the genus *Microsetella* currently consists of two documented species with evidence of local adaptation to, for example, temperature (Barth-Jensen et al. 2020), oncaeids include > 100 species that occupy both different geographic areas and different water depths (Böttger-Schnack and Schnack 2013). Furthermore, as *M. norvegica* is common at salinities down to 25 ppm (Koski et al. 2021), it appears somewhat more tolerant to lower salinity than *Triconia* spp., and therefore also dominates fjord ecosystems and coastal areas (Arendt et al. 2013). Both *M. norvegica* and *Triconia* spp. rely on marine snow as a food source and tend to have similar feeding rates at 0.1–0.4 μg C $ind.^{-1}$ d^{-1} (Koski et al. 2020), thus climate change with altered seasonal temperature, salinity, and stratification cycles, may have different effects on these two species. Nevertheless, these two copepod genera are numerically dominating in many different types of ecosystems (Nishibe and Ikeda 2007; Svensen et al. 2018) and their functional similarities suggests that the aggregate degradation rates estimated for *M. norvegica* can also be representative for copepods within the Oncaeidae family. This indicates that small harpacticoids and oncaeids may have a larger impact on the downward flux regulation than calanoids. Due to high surface abundance in coastal ecosystems, active behavior toward finding, and feeding on aggregates such as marine snow, we suggest that *M. norvegica* may be considered one of the most efficient gatekeepers for carbon fluxes in the surface oceans.

Data availability statement

Hydrographical data are available at https://dataverse.no/dataverse/nmdc. The following datasets are available through the links provided in parenthesis: phytoplankton community composition (https://doi.org/10.15468/s67dzx); abundance of *Microsetella norvegica* (https://doi.org/10.15468/kytcry); zooplankton community composition (https://doi.org/10.15468/ss52m7); downward flux of Chl *a*, POC, PON, and C : N ratios (https://doi.org/10.11582/2023.00063); suspended concentrations of Chl *a*, POC, PON (https://doi.org/10.11582/2023.00064); and the VPR data (https://doi.org/10.11582/2023.00062).

References

Alldredge, A. L. 1972. Abandoned larvacean houses: A unique food source in the pelagic environment. Science **177**: 885–887.

Alldredge, A. L., and M. W. Silver. 1988. In situ settling behaviour of marine snow. Limnol. Oceanogr. **33**: 339–351.

Alldredge, A. L., and G. A. Jackson. 1995. Aggregation in marine systems. Deep-Sea Res. **42**: 1–7.

Arendt, K. E., T. Juul-Pedersen, J. Mortensen, M. E. Blicher, and S. Rysgaard. 2013. A 5-year study of seasonal patterns in mesozooplankton community structure in a sub-Arctic fjord reveals dominance of *Microsetella norvegica* (Crustacea, Copepoda). J. Plankton Res. **35**: 105–120.

Baker, C. A., M. L. Estapa, M. Iversen, R. Lampitt, and K. Buesseler. 2020. Are all sediment traps created equal? An intercomparison study of carbon export methodologies at the PAP-SO site. Prog. Oceanogr. **184**: 102317.

Barth-Jensen, C., and others. 2020. Temperature-dependent egg production and egg hatching rates of small egg-carrying and broadcast-spawning copepods *Oithona similis*, *Microsetella norvegica* and *Microcalanus pusillus*. J. Plankton Res. **42**: 564–580.

Belcher, A., M. Iversen, C. Manno, S. A. Henson, G. A. Tarling, and R. Sanders. 2016. The role of particle associated microbes in remineralization of fecal pellets in the upper mesopelagic of the Scotia Sea, Antarctica. Limnol. Oceanogr. **61**: 1049–1064.

Böttger-Schnack, R., and D. Schnack. 2013. Definition of species groups of Oncaeidae (Copepoda: Cyclopoida) as basis for a worldwide identification key. J. Nat. Hist. **47**: 265–288.

Briggs, N., G. Dall'Olmo, and H. Claustre. 2020. Major role of particle fragmentation in regulating biological sequestration of CO_2 by the oceans. Science **367**: 791–793.

Buesseler, K. O., and others. 2007. An assessment of the use of sediment traps for estimating upper ocean particle fluxes. J. Mar. Res. **65**: 345–416.

Cawley, G. F., M. Décima, A. Mast, and J. C. Prairie. 2021. The effect of phytoplankton properties on the ingestion of marine snow by *Calanus pacificus*. J. Plankton Res. **43**: 957–973.

Coppola, L., M. Roy-Barman, P. Wassmann, S. Mulsow, and C. Jeandel. 2002. Calibration of sediment traps and particulate organic carbon export using ^{234}Th in the Barents Sea. Mar. Chem. **80**: 11–26.

Dugas, J. C., and J. A. Koslow. 1984. *Microsetella norvegica*—A rare report of a potentially abundant copepod on the Scotian shelf. Mar. Biol. **84**: 131–134.

Dutz, J., M. Koski, and S. H. Jónasdóttir. 2008. Copepod reproduction is unaffected by diatom aldehydes or lipid composition. Limnol. Oceanogr. **53**: 225–235.

Edler, L. 1979. Recomendations for marine biological studies in the Baltic Sea; phytoplankton and chlorophyll. Baltic Marine Biologists. University of Stockholm.

Eilertsen, H. C., B. Schei, and J. P. Taasen. 1981. Investigations on the plankton community of Balsfjorden, northern Norway: The phytoplankton 1976–1978. Abundance, species composition and succession. Sarsia **66**: 129–141.

Eilertsen, E., and J. P. Taasen. 1984. Investigations of the plankton community of Balsfjorden, Northern Norway. The phytoplankton 1976–1978. Environmental factors, dynamics of growth, and primary production. Sarsia **69**: 1–15.

Eilertsen, H. C., and J. Skardhamar. 2006. Temperatures of north Norwegian fjords and coastal waters: Variability, significance of local processes and air-sea heat exchange. Estuar. Coast. Shelf Sci. **67**: 530–538.

Falk-Petersen, S., and C. C. E. Hopkins. 1981. Ecological investigations on the zooplankton community of Balsfjorden, northern Norway: Population dynamics of the euphausiids *Thysanoessa inermis* (Kroyer), *Thysanoessa raschii* (M. Sars) and *Meganyctiphanes norvegica* (M. Sars) in 1976 and 1977. J. Plankton Res. **3**: 177–192.

Fowler, S. W., and G. A. Knauer. 1986. Role of large particles in the the transport of elements and organic compounds through the ocean water column. Prog. Oceanogr. **16**: 147–194.

Frost, B. W., and N. C. Franzen. 1992. Grazing and iron limitation in the control of phytoplankton stock and nutrient concentration: A chemostat analogue of the Pacific equatorial upwelling zone. Mar. Ecol. Prog. Ser. **83**: 291–303.

Green, E. P., and M. J. Dagg. 1997. Mesozooplankton associations with medium to large marine snow aggregates in the northern Gulf of Mexico. J. Plankton Res. **19**: 435–447.

Holling, C. 1966. The functional response of invertebrate predators to prey density. Mem. Entomol. Soc. Canada **98**: 5–86.

Holm-Hansen, O., C. J. Lorenzen, R. W. Holmes, and J. D. H. Strickland. 1965. Fluorometric determination of chlorophyll. J. Cons. Int. Explor. Mer. **30**: 3–15.

Iversen, M. H. 2023. Carbon export in the ocean: A biologist's perspective. Ann. Rev. Mar. Sci. **15**: 357–381.

Iversen, M. H., and L. K. Poulsen. 2007. Coprorhexy, coprophagy, and coprochaly in the copepods *Calanus helgolandicus*, *Pseudocalanus elongatus*, and *Oithona similis*. Mar. Ecol. Prog. Ser. **350**: 79–89.

Iversen, M. H., N. Nowald, H. Ploug, G. A. Jackson, and G. Fischer. 2010. High resolution profiles of vertical particulate organic matter export off Cape Blanc, Mauritania: Degradation processes and ballasting effects. Deep-Sea Res. I Oceanogr. Res. Pap. **57**: 771–784.

Jackson, G. A. 1993. Flux feeding as a mechanism for zooplankton grazing and its implications for vertical particulate flux Limnol. Oceanography **38**: 1328–1331.

Jackson, G. A., and D. M. Checkley. 2011. Particle size distributions in the upper 100 m water column and their implications for animal feeding in the plankton. Deep-Sea Res. I Oceanogr. Res. Pap. **58**: 283–297.

Kiørboe, T. 2000. Colonization of marine snow aggregates by invertebrate zooplankton: Abundance, scaling, and possible role. Limnol. Oceanogr. **45**: 479–484.

Kiørboe, T. 2001. Formation and fate of marine snow: Small-scale processes with large-scale implications. Sci. Mar. **65**: 57–71.

Kiørboe, T. 2011. How zooplankton feed: Mechanisms, traits and trade-offs. Biol. Rev. **86**: 311–339.

Koski, M., T. Kiørboe, and K. Takahashi. 2005. Benthic life in the pelagial: Aggregate encounter and degradation rates by pelagic harpacticoid copepods. Limnol. Oceanogr. **50**: 1254–1263.

Koski, M., E. Møller, M. Maar, and A. W. Visser. 2007. The fate of discarded appendicularian houses: Degradation by the copepod, *Microsetella norvegica*, and other agents. J. Plankton Res. **29**: 641–654.

Koski, M., J. Boutorh, and C. de la Rocha. 2017. Feeding on dispersed vs. aggregated particles: The effect of zooplankton feeding behavior on vertical flux. PLoS One **12**: e0177958.

Koski, M., B. Valencia, R. Newstead, and C. Thiele. 2020. The missing piece of the upper mesopelagic carbon budget? Biomass, vertical distribution and feeding of aggregate-associated copepods at the PAP site. Prog. Oceanogr. **181**: 102243.

Koski, M., R. Swalethorp, S. Kjellerup, and T. G. Nielsen. 2021. Aggregate-colonizing copepods in a glacial fjord: Population dynamics, vertical distribution and allometric scaling of growth and mortality rates of *Microsetella norvegica* and *Oncaea* spp. Prog. Oceanogr. **197**: 102670.

Koski, M., and F. Lombard. 2022. Functional responses of aggregate-colonizing copepods. Limnol. Oceanogr. **67**: 2059–2072.

Kwasniewski, S., and others. 2010. The impact of different hydrographic conditions and zooplankton communities on provisioning Little Auks along the West coast of Spitsbergen. Prog. Oceanogr. **87**: 72–82.

Lampitt, R. S., K. F. Wishner, C. M. Turley, and M. V. Angel. 1993. Marine snow studies in the northeast Atlantic Ocean—Distribution, composition and role as a food source for migrating plankton. Mar. Biol. **116**: 689–702.

Lombard, F., M. Koski, and T. Kiørboe. 2013. Copepods use chemical trails to find sinking marine snow aggregates. Limnol. Oceanogr. **58**: 185–192.

Marsay, C. M., R. J. Sanders, S. A. Henson, K. Pabortsava, E. P. Achterberg, and R. S. Lampitt. 2015. Attenuation of sinking particulate organic carbon flux through the mesopelagic ocean. Proc. Natl. Acad. Sci. USA **112**: 1089–1094.

Mayor, D. J., W. C. Gentleman, and T. R. Anderson. 2020. Ocean carbon sequestration: Particle fragmentation by copepods as a significant unrecognised factor? Explicitly representing the role of copepods in biogeochemical models may fundamentally improve understanding of future ocean carbon storage. Bioessays **42**: e2000149.

Mooney, B. P., M. H. Iversen, and M. F. Norrbin. 2023. Impact of *Microsetella norvegica* on carbon flux attenuation and as a secondary producer during the polar night in the subarctic Porsangerfjord. Front. Mar. Sci. **10**: 996275.

Nishibe, Y., and T. Ikeda. 2007. Vertical distribution, population structure and life cycles of four oncaeid copepods in the Oyashio region, western subarctic Pacific. Mar. Biol. **150**: 609–625.

Norrbin, M. F., C. S. Davis, and S. M. Gallager. 1996. Differences in fine-scale structure and composition of zooplankton between mixed and stratified regions of Georges Bank. Deep-Sea Res. II Top. Stud. Oceanogr. **43**: 1905–1924.

Ploug, H., M. H. Iversen, M. Koski, and E. T. Buitenhuis. 2008. Production, oxygen respiration rates, and sinking velocity of copepod fecal pellets: Direct measurements of ballasting by opal and calcite. Limnol. Oceanogr. **53**: 469–476.

Reigstad, M., C. Wexels Riser, and C. Svensen. 2005. Fate of copepod faecal pellets and the role of *Oithona*. Mar. Ecol. Prog. Ser. **304**: 265–270.

Sameoto, D., and others. 2000. Collecting zooplankton, p. 684. *In* R. P. Harris, P. H. Wiebe, J. Lenz, H. R. Skjoldal, and M. Huntley [eds.], ICES zooplankton methodology manual. Academic Press.

Simon, M., A. L. Alldredge, and F. Azam. 1990. Bacterial carbon dynamics on marine snow. Mar. Ecol. Prog. Ser. **65**: 205–211.

Steinberg, D. K., B. A. S. Van Mooy, K. O. Buesseler, P. W. Boyd, T. Kobari, and D. M. Karl. 2008. Bacterial vs. zooplankton control of sinking particle flux in the ocean's twilight zone. Limnol. Oceanogr. **53**: 1327–1338.

Stukel, M. R., M. D. Ohman, T. B. Kelly, and T. Biard. 2019. The roles of suspension-feeding and flux-feeding zooplankton as gatekeepers of particle flux into the Mesopelagic Ocean in the Northeast Pacific. Front. Mar. Sci. **6**: 397.

Svensen, C., and T. Kiørboe. 2000. Remote prey detection in *Oithona similis*: Hydromechanical versus chemical cues. J. Plankton Res. **22**: 1155–1166.

Svensen, C., L. Seuthe, Y. Vasilyeva, A. Pasternak, and E. Hansen. 2011. Zooplankton distribution across Fram Strait in autumn: Are small copepods and protozooplankton important? Prog. Oceanogr. **91**: 534–544.

Svensen, C., C. W. Riser, M. Reigstad, and L. Seuthe. 2012. Degradation of copepod faecal pellets in the upper layer: Role of microbial community and *Calanus finmarchicus*. Mar. Ecol. Prog. Ser. **462**: 39–49.

Svensen, C., M. T. Antonsen, and M. Reigstad. 2018. Small copepods matter: Population dynamics of *Microsetella norvegica* in a high-latitude coastal ecosystem. J. Plankton Res. **40**: 446–457.

Tamelander, T., A. B. Aubert, and C. W. Riser. 2012. Export stoichiometry and contribution of copepod faecal pellets to vertical flux of particulate organic carbon, nitrogen and phosphorus. Mar. Ecol. Prog. Ser. **459**: 17–28.

Trudnowska, E., K. Blachowiak-Samolyk, and L. Stemmann. 2023. Structures of coexisting marine snow and zooplankton in coastal waters of Svalbard (European Arctic). Elementa Sci. Anthrop. **11**: 00010.

Turner, J. T. 2002. Zooplankton fecal pellets, marine snow and sinking phytoplankton blooms. Aquat. Microb. Ecol. **27**: 57–102.

Turner, J. T. 2004. The importance of small planktonic copepods and their roles in pelagic marine food webs. Zool. Stud. **43**: 255–266.

Utermöhl, H. 1958. Zur vervollkommnung der quantitativen phytoplankton methodik. Verh. Int. Verein. Limnol. **9**: 1–38.

Uye, S., I. Aoto, and T. Onbé. 2002. Seasonal population dynamics and production of *Microsetella norvegica*, a widely distributed but little-studied marine planktonic harpacticoid copepod. J. Plankton Res. **24**: 143–153.

van der Jagt, H., I. Wiedmann, N. Hildebrandt, B. Niehoff, and M. H. Iversen. 2020. Aggregate feeding by the copepods *Calanus* and *Pseudocalanus* controls carbon flux attenuation in the Arctic Shelf Sea during the productive period. Front. Mar. Sci. **7**: 543124.

Visser, A. W., and P. R. Jonsson. 2000. On the reorientation of non-spherical prey particles in a feeding current. J. Plankton Res. **22**: 761–777.

Acknowledgments

We thank the crew at R/V "Johan Ruud" for help at sea and Ulrike Grothe and Christine Dybwad for assistance during fieldwork and experiments. This work was supported by the Fram Center flagship "Climate Change in Fjord and Coast" grant nr 2019147470 292018. IW's contribution was funded by ARCEx, the Research Centre for Arctic Petroleum Exploration (Norwegian Research Council #228107 and industry partners). CS and MK has received funding from the European Union's Horizon 2020 research and innovation program under grant agreement no. 869383. MHI was supported by the DFG-Research Center/Cluster of Excellence "The Ocean in the Earth System": EXC-2077-390741603 and the HGF Infrastructure Program FRAM of the Alfred Wegener Institute, Helmholtz Center for Polar and Marine Research. The publication charges for this article have been funded by the publication fund of UiT The Arctic University of Norway.

Conflict of Interest

None declared.

Submitted 27 April 2023
Revised 21 December 2023
Accepted 08 July 2024

Associate editor: Michael R. Stukel